

Radiofrequency encoded angular-resolved light scattering

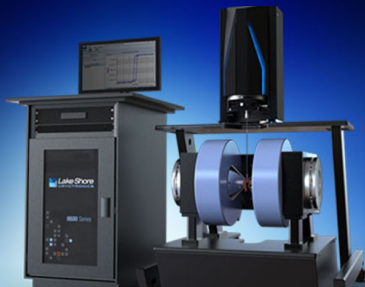
Brandon W. Buckley¹, Najva Akbari¹, Eric D. Diebold¹, Jost Adam, and Bahram Jalali¹

Citation: *Appl. Phys. Lett.* **106**, 123701 (2015); doi: 10.1063/1.4915621

View online: <http://dx.doi.org/10.1063/1.4915621>

View Table of Contents: <http://aip.scitation.org/toc/apl/106/12>

Published by the [American Institute of Physics](#)



NEW 8600 Series VSM

For fast, highly sensitive
measurement performance

LEARN MORE 

Radiofrequency encoded angular-resolved light scattering

Brandon W. Buckley,^{1,2,a)} Najva Akbari,^{2,a)} Eric D. Diebold,^{2,3,4,a)} Jost Adam,^{2,4,5}
 and Bahram Jalali^{2,3,4,6,b)}

¹*Department of Physics, University of California Los Angeles, 420 Westwood Plaza, Los Angeles, California 90095, USA*

²*Department of Electrical Engineering, University of California Los Angeles, 420 Westwood Plaza, Los Angeles, California 90095, USA*

³*Department of Bioengineering, University of California Los Angeles, 420 Westwood Plaza, Los Angeles, California 90095, USA*

⁴*California NanoSystems Institute, University of California Los Angeles, 420 Westwood Plaza, Los Angeles, California 90095, USA*

⁵*The Mads Clausen Institute, University of Southern Denmark, Alsion 2, DK-6400 Sønderborg, Denmark*

⁶*Department of Surgery, David Geffen School of Medicine, University of California Los Angeles, 420 Westwood Plaza, Los Angeles, California 90095, USA*

(Received 25 September 2014; accepted 10 March 2015; published online 23 March 2015)

The sensitive, specific, and label-free classification of microscopic cells and organisms is one of the outstanding problems in biology. Today, instruments such as the flow cytometer use a combination of light scatter measurements at two distinct angles to infer the size and internal complexity of cells at rates of more than 10 000/s. However, by examining the entire angular light scattering spectrum, it is possible to classify cells with higher resolution and specificity. Current approaches to performing these angular spectrum measurements all have significant throughput limitations, making them incompatible with other state-of-the-art flow cytometers. Here, we introduce a method for performing complete angular scattering spectrum measurements at high throughput combining techniques from the field of scattering flow-cytometry and radiofrequency communications. Termed Radiofrequency Encoded Angular-resolved Light Scattering, this technique multiplexes angular light scattering in the radiofrequency domain, such that a single photodetector captures the entire scattering spectrum from a particle over approximately 100 discrete incident angles on a single shot basis. As a proof-of-principle experiment, we use this technique to perform scattering measurements over a range of 30° from a tapered optical fiber at a scan rate of 250 kHz. © 2015 AIP Publishing LLC. [<http://dx.doi.org/10.1063/1.4915621>]

The angular light scattering spectrum of biological cells and microscopic particles encodes significant information of their biochemical structure and morphological properties, such as size, shape, index of refraction, and internal complexity.¹ Scattering measurements, such as those used in flow cytometers for particle classification, typically only measure scattering amplitudes at two angles: forward (0°) and side (90°) scatter. Although capable of operating at high-throughput, such systems fail to recover much of the detailed information contained in the full scattering profile and therefore suffer from limited particle differentiation. Instruments exist which can resolve the full angular scattering profile, via scanning flow cytometry (SFC), such as the mechanical scanning or goniometric approach,² flying light scattering indicatrix (FLSI) method,^{3,4} and the liquid-core-waveguide based method.⁵ Though these approaches provide more information than standard techniques, they all suffer from speed limitations—none approaching the throughputs of standard flow cytometers—and are typically hindered in dynamic range due to the large discrepancy in the number of photons scattered in the forward and steep side scattering angles.

A recently developed technique, termed Spectrally Encoded Angular-resolved Light Scattering (SEALS), addresses this full-spectrum scattering measurement problem in a high throughput fashion using an ultrafast optical approach.⁶ Inspired by a high-throughput bright field imaging technique, Serial Time Encoded Amplified Microscopy (STEAM),⁷ SEALS uses a one-to-one scatter angle-to-optical wavelength mapping to encode the angular scattering profile onto the spectrum of a broadband ultrafast optical pulse. Using the dispersive Fourier transform (DFT)⁸ and a single high speed photodetector, an entire angular scattering spectrum can be read on a single shot basis in real time at MHz repetition rates. Additionally, using a digitally programmable optical filter, SEALS pre-equalizes the intensity of the optical spectrum to compensate for the discrepancy in scattering intensities between forward and side scattered light, improving the system dynamic range. While SEALS measures scattering spectra with high dynamic range at MHz readout rates, this performance comes with the cost of system complexity. The reliance on a mode-locked laser and dispersive optics, in particular, limit the usefulness of SEALS to only the most bandwidth intensive applications.

Here, we introduce a multi-angle resolved light scattering measurement technique, which, like SEALS, is inspired by a high-speed imaging method: Fluorescence Imaging Using Radio-frequency Tagged Emission (FIRE).⁹ Similar to

^{a)}B. W. Buckley, N. Akbari, and E. D. Diebold contributed equally to this work.

^{b)}Author to whom correspondence should be addressed. Electronic mail: jalali@ucla.edu

how SEALS encodes the angular scattering profile into the spectrum of a broadband optical pulse, this technique, termed Radio-frequency Encoded Angular-resolved Light Scattering (REALS), uses a one-to-one radiofrequency-to-angle mapping of a continuous wave (CW) laser to encode the scattering profile into the radio-frequency (RF) domain. Upon detection by a single-pixel photomultiplier tube (PMT), the scattering profile can be recovered using an electrical spectrum analyzer (ESA) or the signal can be digitized and analyzed in real-time using digital frequency domain techniques such as the fast Fourier transform (FFT). REALS achieves broadband operation through radio-frequency domain multiplexing, and with digital pre-equalization of the RF intensities, REALS can achieve large dynamic range across the full angular distribution. Additionally, REALS is implemented using conventional optics and RF acousto-optic (AO) devices, adding to its simplicity and robustness.

Figure 1 shows the operational principles of REALS. Radiofrequency-encoded light is incident on a sample from multiple discrete angles, and a single-element detector detects the scattered light from a single position. In this fashion, the radiofrequency components of the resulting photodetector signal are equivalent to the angular scattering spectrum of the sample. Equivalently, by illuminating the sample with light incident at multiple transverse optical k -vectors (k_{RF}) and detecting the light scattered into a single direction (k_{PMT}) enable a measurement of the spatial frequencies of the sample (k_{sample}). To generate the radiofrequency-encoded light incident upon the sample at a range of discrete angles, a CW laser is first split into two beams using a Mach-Zehnder interferometer. The beam in the first arm is diffracted into multiple beams (RF beams) using a wide bandwidth AO deflector (AOD), driven by a radiofrequency comb produced by direct digital synthesis (DDS).⁹ The time-bandwidth product (TBP) of the AOD dominates the angular resolution of the system. Through the acousto-optic interaction, diffracted optical beams are shifted in both output angle and optical frequency by the corresponding comb line frequencies. This frequency comb

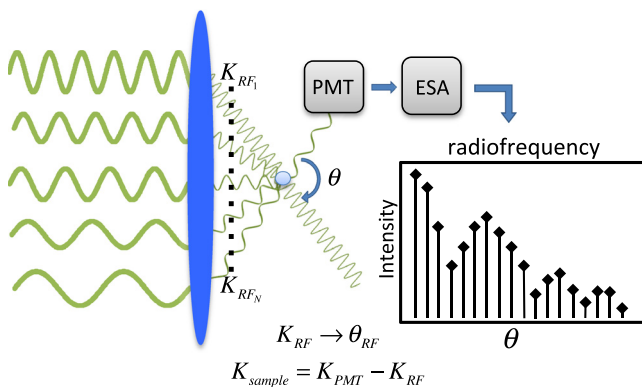


FIG. 1. Operational principle of REALS. Radiofrequency-encoded light, generated via an acousto-optic interaction, is directed to a scattering sample at a range of transverse wavevectors K_{RF} using a lens. A photomultiplier tube detects light scattered from the sample, and an electrical spectrum analyzer is used to quantify the radiofrequency content of the detected signal. Given the angle of the PMT (K_{PMT}) and the RF-to angle mapping spectrum (K_{RF}), the 2D scattering spectrum of the sample (K_{sample}) is measured in a single shot without scanning.

digitally phase-engineered using a Golay complementary sequence in order to minimize its peak to average power ratio¹⁰ to avoid RF saturation in the AOD. The second arm of the interferometer uses an AO frequency shifter (AOFS) to produce a local oscillator (LO) beam to heterodyne the scattering signals and produce beat frequencies in a desired portion of the RF spectrum—either near baseband or in a noise free passband. A non-polarizing beamsplitter combines the RF and LO beams, and a tube lens and objective lens direct the RF and LO beams to the sample over a range of angles. Light scattered by the sample is detected by a photomultiplier tube-based detector module consisting of two pinholes, for angular selectivity, and a high dynamic range PMT (20% quantum efficiency at 532 nm, 10^6 gain, and 10 nA dark current, Hamamatsu R3896). This two-pinhole configuration, along with the AOD TBP, determines the angular resolution of the REALS technique, as the size and spacing of the pinholes can be adjusted to alter the angular resolution of the system, while allowing more or less light into the PMT. The PMT output signals are lowpass filtered and amplified by a 500-MHz bandwidth low noise amplifier and are analyzed by either an electrical spectrum analyzer or a digitizing oscilloscope and subsequent FFT-based signal processing. Figure 2 shows a schematic of the REALS system.

To quantify the system performance, we first verified the existence of a one-to-one RF-to-angle mapping and measured the angular resolution and range. This demonstration of REALS employed a longitudinal mode TeO₂ AOD driven with a 1 MHz spaced RF comb from 305 MHz to 395 MHz. A LO beam of 200.5 MHz was chosen so as to avoid the drive frequencies and intra-comb beat-frequencies from interfering with the heterodyne signal at the PMT. With a beam diameter of 2.2 mm at the entrance of the AOD, the TBP of this configuration was ~ 48 . Two 100- μm pinholes spaced by 6 cm were aligned with the entrance of the detector on a rotation stage at the eucentric position and the detected frequency components were monitored as a function of detector angle. Using a 40 \times , 0.66-NA objective lens collimated light signals were collected over a range of 30 $^\circ$, generating a linear mapping of 0.34 $^\circ$ /MHz. The angular

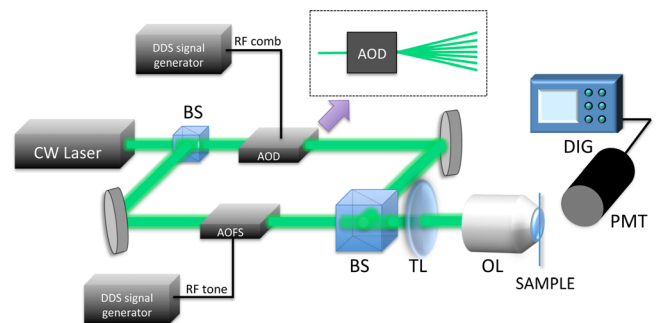


FIG. 2. Schematic of the REALS system. A 532-nm CW laser is split into two arms of a Mach-Zehnder interferometer containing two AO devices. The acousto-optic deflector creates multiple frequency-shifted beams in the RF comb arm, which are diffracted at unique angles. These beams are directed to the sample via a tube and objective lens, illuminating the sample from a range of angles. The AOFS generates an LO beam which scatters off of the sample and beats with the scattered RF beams at the detector. The beat signals are detected by a PMT and recorded by a digitizing oscilloscope.

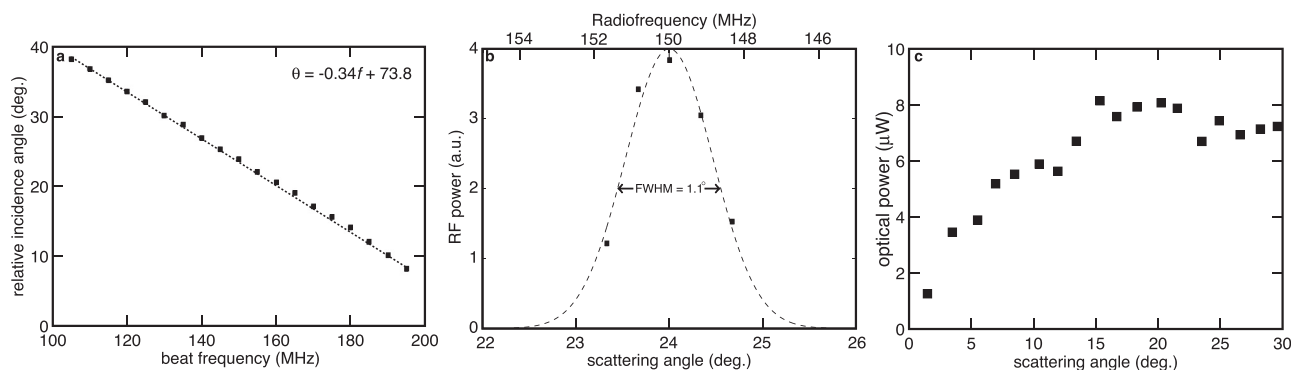


FIG. 3. REALS RF-to-angle mapping, angular resolution, and optical power versus scattering angle. (a) Rotating the angular position of the PMT detector module about the focus point provides a measurement of the RF-to-angle mapping of REALS. (b) Using this mapping as calibration, the angular resolution of the system can be determined using a Gaussian fit to the data at a single angle. (c) The non-uniform efficiency of the AOD is exploited here to maximize optical power at high scattering angles and reduce the power at low scattering angles in order to provide pre-equalization and dynamic range improvement.

resolution of this configuration was 1.1° (3.48 MHz)— ~ 26 resolved points. The reduction in resolved points as compared to the TBP of 48 of the AOD can be explained by the additional divergence of the collimated beams after the objective lens as well as the finite aperture size of the pinholes. In order to maximize the dynamic range of the system, the angle-to-RF mapping was chosen such that the intrinsic variation in diffraction efficiency of the AOD equalized the variation in forward and large-angle scattering amplitudes. The results of these system performance characterization measurements are shown in Figure 3.

To demonstrate the ability of REALS to distinguish scattering from samples of various sizes, we examined the scattering spectra from a tapered optical fiber at various locations along the taper. A fiber was chosen as the most appropriate sample for this proof-of-principle demonstration due to its cylindrical symmetry, in lieu of, for example, a static sample mounted on a glass slide. For interrogating particles

in flow—one potential high-impact application of REALS—a micro-fluidic flow channel with similar cylindrical symmetry would be ideal so as to avoid refraction from minimizing the angular range of the incident RF-shifted beams as well as from distorting the scattering spectrum. To produce the tapered fiber sample, a single mode optical fiber (SMF-28) was heated to its softening point in a hydrogen flame and pulled at a uniform velocity using two linear translation stages.¹¹ The fiber taper was attached to a rigid mount and placed at the focal plane of the objective lens. The PMT detector was placed in line with the LO beam at the forward scatter angle. Over the range of probed positions, the fiber diameter tapered from approximately $20\ \mu\text{m}$ to $5\ \mu\text{m}$. Using the digitizing oscilloscope, scattering spectra were recorded from each probed position at a rate of 250 kHz, using a frequency comb spacing of 1 MHz. Figure 4 shows the mean and standard deviation of 200 scatterer measurements fitted to simulated Mie scattering profiles.¹²

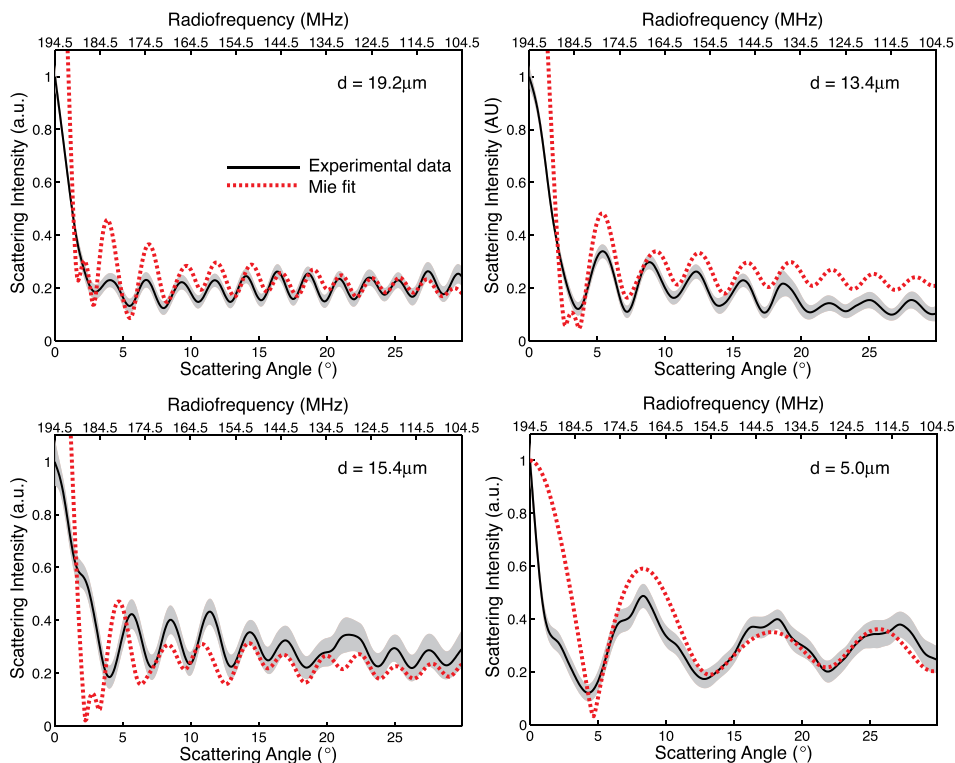


FIG. 4. Scattering from a tapered silica optical fiber in air. These scattering profiles show the angular scattering spectrum from different locations on the taper, each measured at a rate of 250 000 spectra per second. These plots represent the mean (dark solid line) and standard deviation (gray shaded area) of 200 individual spectra. Each spectrum is taken using 91 discrete radiofrequencies. Mie scattering profiles were simulated and cylindrical diameters determined to best fit the measured scattering data. The diameters found with simulations match closely those of the tapered fiber sample, validating the ability of REALS to discern morphological structure from the scattering profile at high-speed and with high-resolution.

In this implementation of REALS, the single LO beam is focused through the objective along with the angularly diffracted beams and is captured by the detector at the forward scattering angle. The final mirror of the LO beam path can be translated in order to adjust its angular incidence on the sample to align with the PMT and optimize the modulation depth of the beat signal. All of the radio-frequency beams interfere with each other at the PMT, so the RF-comb and LO frequencies were chosen to keep the desired signal away from any other interfering signals. While this demonstration utilized the intrinsic diffraction efficiency variation of the AOD to compensate for the difference in small- and large-angle scattering amplitudes to improve dynamic range, the digitally synthesized nature of REALS enables the use of more flexible digital pre-equalization as well.

The proof-of-principle scattering measurements shown in Figure 4 demonstrate the ability to resolve small changes in diameter from a dielectric scattering object. As the diameter decreases, the width of the lobes in the scattering spectra increases, as predicted by classical Mie theory. This measurement was taken at a rate of 250 kHz, which is well above the requisite data acquisition rate for modern flow cytometers ($\sim 10\,000$ events per second). Integration of REALS with a suitable flow channel will enable rapid, label-free scattering-based classification of cells, which could prove useful for many applications, including stem cell research,¹³ clinical diagnostics,^{14–17} and high-resolution analysis of cellular sub-populations.^{18,19} The current REALS system has 1.1° (3.48 MHz) scattering resolution over the 91-MHz RF bandwidth (~ 26 resolved scattering angles) and a 30° range. The performance can be significantly improved by using higher-resolution AODs²⁰ (with larger apertures and wider bandwidths), smaller detector pinholes, and higher NA objective lenses, for applications requiring higher angular resolution or to collect scattering spectra over a larger angular range.

Due to its use of RF multiplexing and a single PMT for readout, REALS provides fast, sensitive, and high-resolution measurements of the angular scattering spectra of

microscopic objects. When implemented in a flow-cytometry system, REALS may ultimately prove to be the method of choice for high-throughput, label-free, high-resolution particle classification using optical scattering.

¹Y.-L. Pan, M. J. Berg, S. S.-M. Zhang, H. Noh, H. Cao, R. K. Chang, and G. Videa, *Cytometry A* **79A**, 284 (2011).

²E. Marx and G. W. Mulholland, *J. Res. Natl. Bur. Stand.* **88**, 321 (1983).

³J. T. Soini, A. V. Chernyshev, P. E. Hänninen, E. Soini, and V. P. Maltsev, *Cytometry* **31**, 78 (1998).

⁴A. V. Chernyshev, V. I. Prots, A. A. Doroshkin, and V. P. Maltsev, *Appl. Opt.* **34**(27), 6301–6305 (1995).

⁵K. Singh, C. Capjack, W. Rozmus, and C. J. Backhouse, *IEE Proc. Nanobiotechnol.* **153**, 135 (2006).

⁶J. Adam, A. Mahjoubfar, E. D. Diebold, B. W. Buckley, and B. Jalali, *Opt. Express* **21**, 28960 (2013).

⁷K. Goda, K. K. Tsia, and B. Jalali, *Nature* **458**, 1145 (2009).

⁸K. Goda and B. Jalali, *Nat. Photonics* **7**, 102 (2013).

⁹E. D. Diebold, B. W. Buckley, D. R. Gossett, and B. Jalali, *Nat. Photonics* **7**, 806 (2013).

¹⁰X. Huang, “Simple implementations of mutually orthogonal complementary sets of sequences,” in *Proceedings of the 2005 International Symposium on Intelligent Signal Processing and Communication Systems* (IEEE, 2005), pp. 369–372.

¹¹R. R. Gattass, G. T. Svacha, L. Tong, and E. Mazur, *Opt. Express* **14**, 9408 (2006).

¹²*Absorption and Scattering of Light by Small Particles*, edited by C. F. Bohren and D. R. Huffman (Wiley-VCH Verlag GmbH, Weinheim, Germany, 1998).

¹³D. R. Sutherland, L. Anderson, M. Keeney, R. Nayar, and I. Chin-Yee, *J. Hematother.* **5**, 213 (1996).

¹⁴V. Backman, M. B. Wallace, L. T. Perelman, J. T. Arendt, R. Gurjar, M. G. Müller, Q. Zhang, G. Zonios, E. Kline, T. McGillican, S. Shapshay, T. Valdez, K. Badizadegan, J. M. Crawford, M. Fitzmaurice, S. Kabani, H. S. Levin, M. Seiler, R. R. Dasari, I. Itzkan, J. Van Dam, and M. S. Feld, *Nature* **406**, 35 (2000).

¹⁵J. R. Mourant, J. P. Freyer, A. H. Hielscher, A. A. Eick, D. Shen, and T. M. Johnson, *Appl. Opt.* **37**, 3586 (1998).

¹⁶C. Liu, C. Capjack, and W. Rozmus, *J. Biomed. Opt.* **10**, 14007 (2005).

¹⁷K. A. Sem'yanov, P. A. Tarasov, J. T. Soini, A. K. Petrov, and V. P. Maltsev, *Appl. Opt.* **39**, 5884 (2000).

¹⁸D. Zink, A. H. Fischer, and J. A. Nickerson, *Nat. Rev. Cancer* **4**, 677 (2004).

¹⁹X.-T. Su, C. Capjack, W. Rozmus, and C. Backhouse, *Opt. Express* **15**, 10562 (2007).

²⁰J. Eddie, H. Young, and S.-K. Yao, *Proc. IEEE* **69**, 54 (1981).